Synthesis and Dynamic Nuclear Magnetic Resonance Studies of Pentafluorobenzenethiolate Complexes of Molybdenum and Tungsten. The Crystal and Molecular Structures of $[W(SC_6F_5)_3(CO)(\eta^5\text{-}C_5H_5)]\cdot 0.5CH_2Cl_2$ and $[N(PPh_3)_2][Mo(SC_6F_5)_4(\eta^5\text{-}C_5H_5)]$ †

W. A. Wan Abu Bakar, Jack L. Davidson,* W. Edward Lindsell, and Kevin J. McCullough
Department of Chemistry, Heriot-Watt University, Riccarton, Currie, Edinburgh EH14 4AS

The reaction between $[WBr_3(CO)_2(\eta^5\text{-}C_5H_5)]$ and excess of $Tl(SC_6F_5)$ (CH_2Cl_2, 20 °C) affords $Tl[W(SC_6F_5)_4(\eta^5\text{-}C_5H_5)]$ (**2b**) as the major product and $[W(SC_6F_5)_3(CO)(\eta^5\text{-}C_5H_5)]$ (**3**) as the minor product. Complex (**3**) has been structurally characterised as its 0.5 CH_2Cl_2 solvate by *X*-ray diffraction. Chiral molecules of $[W(SC_6F_5)_3(CO)(\eta^5\text{-}C_5H_5)]$ adopt a distorted square-based 'piano-stool' geometry with the *trans* W–S bond [2.443 6(15) Å] longer than the *cis* W–S bonds (mean 2.358 Å). The SC_6F_5 ligands lie with S–C bonds approximately in the plane of the square base and, all C_6F_5 groups have the same rotational orientation about the central W atom. However, dynamic ^{19}F n.m.r. studies of (**3**) reveal that two isomeric forms exist at low temperature due to different orientations of the SC_6F_5 ligands but these undergo exchange at ambient temperature as a result of rotation about the W–SC_6F_5 bonds or inversion at sulphur. Similar studies of complex (**2b**) established that apparent rotation of the SC_6F_5 groups is solvent dependent and occurs in conjunction with ionic dissociation into Tl^+ and $[W(SC_6F_5)_4(\eta^5\text{-}C_5H_5)]^-$. The Tl^I in (**2b**) and related complexes $Tl[Mo(SC_6F_5)_4(\eta^5\text{-}C_5H_5)]$ and $Tl[Mo(SC_6F_5)_2(CO)_2(\eta^5\text{-}C_5H_5)]$ can be replaced by non-co-ordinating cations to give $X^+[M(SC_6F_5)_4(\eta^5\text{-}C_5H_5)]^-$ [M = Mo, X = NBu^n_4 (**4a**) or $N(PPh_3)_2$ (**4b**); M = W, X = NMe_4] and $N(PPh_3)_2^+[Mo(SC_6F_5)_2(CO)_2(\eta^5\text{-}C_5H_5)]^-$ which also exhibit fluxional behaviour according to ^{19}F n.m.r. studies. The structure of complex (**4b**), determined in the solid state by *X*-ray diffraction, comprises discrete ions $[(Ph_3P)N(PPh_3)]^+$ and $[Mo(SC_6F_5)]_4(\eta^5\text{-}C_5H_5)]^-$. The complex anion has a 'piano-stool' geometry with a square base defined by four SC_6F_5 ligands (mean Mo–S 2.420 Å) and the C_6F_5 groups form a 'swastika-like' arrangement about the square plane. Reactions of (**2b**) with tertiary phosphines (L) in CH_2Cl_2 at 20 °C afford 1:2 adducts $Tl[W(SC_6F_5)_4L_2(\eta^5\text{-}C_5H_5)]$ [L = PPh_3 (**6b**), PMe_2Ph (**6c**), or PEt_3 (**6d**)]. Dynamic ^{19}F n.m.r. studies established a different structure for (**6b**) in solution compared to (**6c**) and (**6d**).

Previously we reported that the reaction of $[MoCl(CO)_3(\eta^5\text{-}C_5H_5)]$ with excess of $Tl(SC_6F_5)$ initially affords the novel molybdenum(II)–thallium(I) complex $Tl[Mo(SC_6F_5)_2(CO)_2(\eta^5\text{-}C_5H_5)]$ (**1**) and this reacts further with $Tl(SC_6F_5)$ to give the molybdenum(IV)–thallium(I) derivative $Tl[Mo(SC_6F_5)_4(\eta^5\text{-}C_5H_5)]$ (**2a**).[1] *X*-Ray diffraction studies established that the structure of (**1**) contains an organometallic anion $[Mo(SC_6F_5)_2(CO)_2(\eta^5\text{-}C_5H_5)]^-$ co-ordinated *via* two sulphurs to Tl^I. The latter is further co-ordinated by one *ortho*-fluorine of each C_6F_5 group and, in the solid state, by two sulphurs of another organometallic anion. In contrast (**2a**) comprises discrete molecular units of $Tl[Mo(SC_6F_5)_4(\eta^5\text{-}C_5H_5)]$ in which Tl^I is co-ordinated by four sulphurs and four *ortho*-fluorines, one from each C_6F_5 ring. Thus, the molybdenum, four sulphurs, and four fluorines in complex (**2a**) effectively define a cavity in which the Tl^I is situated. This, and the observation that in solution thallium(I) co-ordination is reversible, raises the possibility that organometallic anions such as (**2a**) may have potential in selective metal-ion sequestration or as metal-ion sensors. With this in mind we have extended our initial studies to cyclopentadienyl tungsten derivatives in addition to carrying out further work on the molybdenum derivatives (**1**) and (**2a**). The results of this work are reported herein.

Results and Discussion

The reaction of $[WCl(CO)_3(\eta^5\text{-}C_5H_5)]$ with excess of $Tl(SC_6F_5)$ in tetrahydrofuran (thf) yields the known[2] tricarbonyl derivative $[W(SC_6F_5)(CO)_3(\eta^5\text{-}C_5H_5)]$. Attempts to substitute the carbonyl ligands with SC_6F_5 were unsuccessful even in refluxing thf, unlike the analogous molybdenum reaction where $Tl[Mo(SC_6F_5)_2(CO)_2(\eta^5\text{-}C_5H_5)]$ (**1**) and $Tl[Mo(SC_6F_5)_4(\eta^5\text{-}C_5H_5)]$ (**2a**) were obtained readily at 20 °C.[1] This may reflect

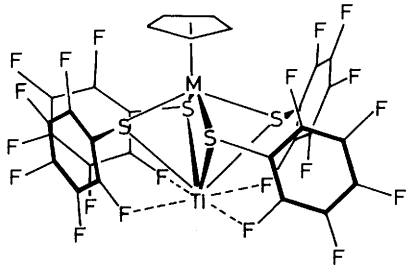

(**2a**) M = Mo
(**2b**) M = W

† Carbonyl(η-cyclopentadienyl)tris(pentafluorobenzenethiolato)tungsten(IV)–dichloromethane (2/1) and bis(triphenylphosphine)iminium (η-cyclopentadienyl)tetrakis(pentafluorobenzenethiolato)molybdate(IV).

Supplementary data available: see Instructions for Authors, *J. Chem. Soc., Dalton Trans.*, 1990, Issue 1, pp. xix—xxii.

Table 1. Fractional co-ordinates of atoms with standard deviations for complex (**3**)

Atom	*x*	*y*	*z*	Atom	*x*	*y*	*z*
W	0.175 40(2)	0.034 10(2)	0.285 88(2)	F(12)	0.632 07(18)	0.091 62(19)	0.224 15(13)
S(1)	0.308 24(16)	0.229 61(13)	0.291 63(11)	C(14)	0.518 24(20)	−0.206 24(16)	0.335 72(14)
S(2)	0.353 24(16)	−0.045 29(13)	0.179 40(11)	C(15)	0.606 94(20)	−0.293 06(16)	0.292 36(14)
S(3)	0.259 69(18)	−0.116 70(15)	0.377 04(11)	C(16)	0.552 41(20)	−0.401 42(16)	0.227 95(14)
C(2)	0.321 11(19)	0.404 69(18)	0.463 32(14)	C(17)	0.409 16(20)	−0.422 96(16)	0.206 91(14)
C(3)	0.283 94(19)	0.513 14(18)	0.523 33(14)	C(18)	0.320 45(20)	−0.336 14(16)	0.250 30(14)
C(4)	0.172 98(19)	0.579 79(18)	0.494 61(14)	C(13)	0.374 99(20)	−0.227 78(16)	0.314 69(14)
C(5)	0.099 17(19)	0.538 01(18)	0.405 86(14)	F(14)	0.571 40(20)	−0.100 63(16)	0.398 50(14)
C(6)	0.136 34(19)	0.429 56(18)	0.345 84(14)	F(15)	0.746 55(20)	−0.272 08(16)	0.312 85(14)
C(1)	0.247 31(19)	0.362 91(18)	0.374 57(14)	F(16)	0.638 85(20)	−0.486 03(16)	0.185 68(14)
F(2)	0.429 25(19)	0.339 73(18)	0.491 32(14)	F(17)	0.356 00(20)	−0.528 57(16)	0.144 15(14)
F(3)	0.355 85(19)	0.553 85(18)	0.609 82(14)	F(18)	0.180 85(20)	−0.357 13(16)	0.229 81(14)
F(4)	0.136 74(19)	0.685 49(18)	0.553 10(14)	C(19)	0.009 8(5)	0.081 1(4)	0.169 2(3)
F(5)	−0.008 97(19)	0.602 98(18)	0.377 86(14)	C(20)	0.029 6(5)	−0.052 7(4)	0.142 1(3)
F(6)	0.064 43(19)	0.388 84(18)	0.259 35(14)	C(21)	−0.013 7(5)	−0.115 1(4)	0.216 2(3)
C(8)	0.351 93(18)	0.112 95(19)	0.042 03(13)	C(22)	−0.060 3(5)	−0.019 9(4)	0.289 2(3)
C(9)	0.412 57(18)	0.202 13(19)	−0.004 07(13)	C(23)	−0.045 8(5)	0.101 4(4)	0.260 2(3)
C(10)	0.547 00(18)	0.254 17(19)	0.026 57(13)	C(24)	0.134 0(7)	0.112 0(6)	0.419 9(5)
C(11)	0.620 79(18)	0.217 00(19)	0.103 29(13)	O	0.109 3(5)	0.154 6(5)	0.496 3(3)
C(12)	0.560 15(18)	0.127 82(19)	0.149 39(13)	Cl(1)	0.032 7(8)	0.372 3(3)	0.008 8(5)
C(7)	0.425 72(18)	0.075 80(19)	0.118 75(13)	Cl(2)	0.023 7(18)	0.631 0(5)	−0.008 9(12)
F(8)	0.220 93(18)	0.062 26(19)	0.012 17(13)	Cl(3)	−0.080(3)	0.609 8(20)	0.022 6(24)
F(9)	0.340 66(18)	0.238 34(19)	−0.078 84(13)	C(25A)	−0.064(4)	0.502 2(17)	0.052 8(21)
F(10)	0.606 09(18)	0.341 07(19)	−0.018 36(13)	C(25B)	0.096(3)	0.477(4)	−0.032(10)
F(11)	0.751 80(18)	0.267 71(19)	0.133 15(13)	C(25C)	−0.068(10)	0.447(4)	0.030(13)

Table 2. Selected derived geometrical parameters (lengths in Å, angles in °) with standard deviations for complex (**3**)

W–S(1)	2.356 1(15)	W–C(23)	2.283(5)
W–S(2)	2.443 6(15)	W–C(24)	2.006(6)
W–S(3)	2.359 4(16)	S(1)–C(1)	1.812 2(24)
W–C(19)	2.329(5)	S(2)–C(7)	1.810 9(24)
W–C(20)	2.376(5)	S(3)–C(13)	1.810(3)
W–C(21)	2.361(5)	C(24)–O	1.142(8)
W–C(22)	2.304(5)		
S(1)–W–S(2)	80.73(5)	C(21)–W–C(24)	107.88(21)
S(1)–W–S(3)	119.75(5)	C(22)–W–C(24)	75.62(21)
S(1)–W–C(24)	85.16(18)	C(23)–W–C(24)	77.93(21)
S(2)–W–S(3)	84.18(5)	W–S(1)–C(1)	112.61(9)
S(2)–W–C(24)	147.03(18)	W–S(2)–C(7)	113.50(9)
S(3)–W–C(24)	77.24(18)	W–S(3)–C(13)	113.47(10)
C(19)–W–C(24)	112.16(21)	W–C(24)–O	178.9(6)
C(20)–W–C(24)	133.02(21)		

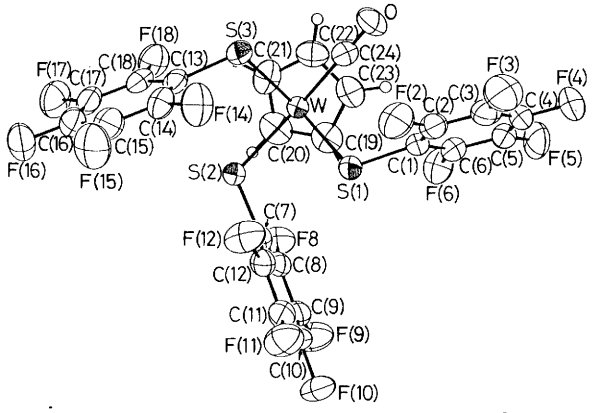

Figure 1. Molecular Structure of $[W(SC_6F_5)_3(CO)(\eta^5\text{-}C_5H_5)]\cdot 0.5\,CH_2Cl_2$ (**3**) (ORTEP[11])

the greater ease with which carbonyl substitution occurs in molybdenum derivatives $[MoX(CO)_3(\eta^5\text{-}C_5H_5)]$.[3] Formation of the tetrathiolate derivative (**2a**) also requires oxidation of the transition metal and consequently the tungsten(IV) derivative $[WBr_3(CO)_2(\eta^5\text{-}C_5H_5)]$ was employed as a precursor to the tungsten analogue (**2b**) in a reaction with $Tl(SC_6F_5)$. The reaction in CH_2Cl_2 at 20 °C readily afforded $Tl[W(SC_6F_5)_4(\eta^5\text{-}C_5H_5)]$ (**2b**) as a yellow powder in 33% yield. However, small quantities (3%) of a dark green air-sensitive crystalline complex (**3**) were also obtained, the counterpart of which was not detected in reactions of $Tl(SC_6F_5)$ with either molybdenum-(II) or -(IV) carbonyl precursors described previously. Complex (**3**) proved too involatile and unstable for mass spectrometric studies but elemental analysis and n.m.r. studies are consistent with the stoicheiometry $[W(SC_6F_5)_3(CO)(\eta^5\text{-}C_5H_5)]\cdot 0.5CH_2Cl_2$ in the solid state. The dichloromethane solvate presumably arises from the purification procedure which involved recrystallisation from CH_2Cl_2–hexane. The i.r. spectrum exhibits a single ν(CO) mode at 2 030 cm^{-1} ($CDCl_3$) whilst the ^1H n.m.r. spectrum contains a dichloromethane signal, in addition to a $\eta^5\text{-}C_5H_5$ singlet. The ^{19}F n.m.r. spectrum at room temperature is more complex and, in particular, is temperature dependent with evidence for more than one isomeric form in solution at low temperatures. Consequently *X*-ray diffraction studies of (**3**) were carried out in order to establish the source of isomerism.

Solid-state Structure of $[W(SC_6F_5)_3(CO)(\eta^5\text{-}C_5H_5)]$ (**3**).—A dark green solvated crystal of complex (**3**), $[W(SC_6F_5)_3(CO)(\eta^5\text{-}C_5H_5)]\cdot 0.5CH_2Cl_2$, suitable for *X*-ray structure analysis was obtained from dichloromethane–hexane solution at −15 °C. In each unit cell of the crystal there are two enantiomers of (**3**) which are well separated (> 3.0 Å) from a highly disordered molecule of CH_2Cl_2. The solid state structure is depicted in Figure 1. Tables 1 and 2, respectively, list atomic fractional co-ordinates and selected, derived geometrical parameters.

The cyclopentadienyl group is bound to W in a typical pentahapto manner and the basic co-ordination geometry around W is a 'piano-stool' with an irregular square base[4] defined by one CO and three SC_6F_5 ligands. A C–C bond of the C_5H_5 ring lies above the π-acceptor CO ligand and the ring is slightly tilted towards this ligand, as found in complexes of

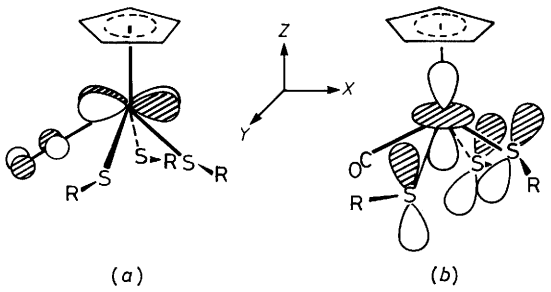

Figure 2. Metal–ligand π interactions in $[W(SC_6F_5)_3(CO)(\eta^5\text{-}C_5H_5)]$ (**3**). (*a*) M d_{xy} (filled), CO π* (empty); (*b*) M d_{z^2} (empty), M p_z (filled)

type $[MX(CO)_3(\eta^5\text{-}C_5H_5)]$.[4] The W–C(carbonyl) bond length [2.006(6) Å] is comparable with bond lengths in cyclopentadienyl tungsten(II) complexes such as $[WCl(CO)_3(\eta^5\text{-}C_5H_5)]$[5] and is not unusually long, contrary to what might be expected if π-back donation to CO was substantially reduced in this formally tungsten(IV) complex; note that in the molybdenum(IV) complex $[MoI_3(CO)_2(\eta^5\text{-}C_5H_4Me)]$ the Mo–C(carbonyl) bonds are significantly longer (mean 2.043 Å).[6] In line with an extended-Hückel molecular orbital (EHMO) analysis by Hoffmann and co-workers[4] of 'piano-stool' molecules the highest occupied molecular orbital (h.o.m.o.) of the formally d^2 complex (**3**) is largely the metal d_{xy} orbital which will bond effectively with the π* orbital of CO as in Figure 2(*a*) and the Cp(centroid)–W–C(carbonyl) angle of 102.6° supports good overlap between these orbitals.

The W–S bond lengths of (**3**) are longer than in the simple tungsten(IV) compound $[W(SBu^t)_4]$ [W–S 2.236(4) Å][7] but within the range of W–S (thiolate) bond lengths for cyclopentadienyl tungsten-(II) to -(V) species.[8] The thiolate ligands, with mean W–S–C angles of 113.2°, are all arranged with S–C bonds lying approximately parallel to the plane of the square base of the 'piano-stool' and this is consistent with Hoffmann's analysis.[4] The π-donor (essentially 3*p*) orbitals of the three SC_6F_5 groups lie perpendicular to the occupied metal d_π orbital and may interact constructively with the lowest unoccupied metal orbital, d_{z^2}, as in Figure 2(*b*). The W–S(2) bond *trans* to the CO ligand is longer [2.4436(15) Å] than the *cis* W–S bonds (mean 2.3578 Å) and this suggests that the CO group causes a *trans* W–S bond weakening. This W–S bond variation can be rationalised in part by the Cp(centroid)–W–S bond angles which are larger (mean 119.9°) for *cis*-SC_6F_5 groups than for *trans*-SC_6F_5 (110.2°) and permit a stronger π interaction with d_{z^2} for the *cis* ligands. These Cp–W–S angles, however, do not result from obvious steric interactions and must themselves be influenced by the W–CO bonding.

All C_6F_5 groups in (**3**) adopt the same rotational orientation about the W–Cp(centroid) axis despite the fact that there appears to be no steric restriction to rotation of the *cis*-C_6F_5–S(3) ligand through 180° towards the CO ligand. The observed structure leaves an unhindered CO ligand in a relatively open co-ordination site and this could facilitate attack, especially if displacement of CO in this 16e complex occurs by an associative mechanism, *e.g.* in the reaction with $Tl(SC_6F_5)$ to form $Tl[W(SC_6F_5)_4(\eta^5\text{-}C_5H_5)]$.

The results of the *X*-ray diffraction study of (**3**) provide a basis for a detailed interpretation of the variable-temperature ^{19}F n.m.r. spectra of the complex. The spectra were recorded over the temperature range −80 to +20 °C in CD_2Cl_2. At 20 °C (see Figure 3) the spectrum contains two distinct sets of *ortho*, *para*, and *meta* signals with relative intensity ratios 2:1 consistent with the presence of one C_6F_5 *trans* to CO and two equivalent *cis*-C_6F_5 groups. Significantly all three *trans* signals are well resolved multiplets whereas the *ortho*- and *meta*-fluorine resonances of the *cis*-C_6F_5 groups are quite broad indicating stereochemical non-rigidity. Before considering the low-temperature spectra we note that three isomeric forms are possible for complex (**3**), that observed in the solid state (**3i**) and two other isomers (**3ii**) and (**3iii**) with one and two C_6F_5 groups respectively rotated by 180° about the M–S bond. In this way sulphur to metal π bonding Figure 2(*b*) will be retained whilst the destabilising antibonding interaction Figure 2(*a*) is minimised. One of us has previously reported evidence for restricted rotation about the W–S bond in $[W(SC_6F_5)(CO)(CF_3C{\equiv}CCF_3)(\eta^5\text{-}C_5H_5)]$ which gives rise to two preferred C_6F_5S orientations where S→M π bonding is optimised.[9] In the present case molecular graphics[10] studies established that isomer (**3iii**) is precluded by severe intramolecular contacts between C_6F_5 groups (b) and (c). In contrast no such constraints are found in isomer (**3ii**). Consequently the observation of two isomeric forms in the ^{19}F n.m.r. spectra at low temperature is consistent with the presence of structures (**3i**) and (**3ii**).

The ^{19}F n.m.r. *para*-fluorine resonances provide the clearest indication of the two isomers as shown in Figure 4. As the temperature is reduced the time-averaged triplet due to the *cis*-C_6H_5 groups broadens and separates into three distinct triplets A, B, and C two of which, B and C, are of approximately equal intensity. At the same time the *trans*-C_6F_5 triplet separates into two triplets D and E the smaller of which E is equivalent in intensity to the two *cis* triplets B and C. Overall integrated intensities indicate that three equal-intensity resonances are present (B, C, and E) while the other two A and D have relative intensity 2:1. The ratio of (B + C + E) to (A + D) is 1.0:1.6. These data indicate that effective rotation of the SC_6F_5 groups about the M–S bonds is relatively fast at room temperature and therefore equilibrates the two forms (**3i**) and (**3ii**) but at lower temperatures such rotation slows to the point where both can be observed. We note at this point that inversion at the pyramidal sulphurs would accomplish the same effect as rotation about the M–S bonds but the data do not distinguish between the two processes. Consequently we shall simplify subsequent discussions by simply referring to the rotational process but the above statement will be implicit. A more detailed interpretation of the n.m.r. data is required since both (**3i**) and (**3ii**) should give rise to three *para*-fluorine resonances at the slow-exchange limit which must occur below −80 °C. It is possible to assign peaks B, C, and E to isomer (**3i**) and A and D to (**3ii**) on the following basis. If we postulate that the C_6F_5S *trans* to CO experiences a lower barrier to rotation than those *cis* to CO such that rotation of the former is still occurring at −80 °C then isomer (**3ii**) will only exhibit two resonances, ratio (*cis*:*trans*) 2:1. This is observed with triplets A and D. We have already noted that isomer (**3iii**) is inaccessible for steric reasons. Thus, although rotation of the *trans*-C_6F_5S in isomer (**3i**) should also have a low electronic barrier the fixed orientation of the *cis*-C_6F_5S ligand will preclude W–SC_6F_5 rotation and therefore result in three distinct C_6F_5 signals, *i.e.* B, C, and E.

Central to this argument is the proposal that the barrier to rotation of the *trans*-C_6F_5S is lower than that of the *cis* groups. This is substantiated by the general appearance of the ^{19}F n.m.r. signals throughout the temperature range studied (see *e.g.* Figure 3) since the *cis*-C_6F_5 resonances are almost invariably much broader than those of the *trans*-C_6F_5 groups. We note, however, that linewidth is not necessarily a guide to the magnitude of rotational barriers since it is a function of both temperature and the chemical shift separation of the exchanging groups at the slow-exchange limit. Despite this the *X*-ray diffraction study of (**3**) supports our proposal since we have already noted that the *trans* M–SC_6F_5 bond length is somewhat longer than those of the *cis*-SC_6F_5 ligands. As discussed earlier this may be a consequence of weaker S→W π donation in the

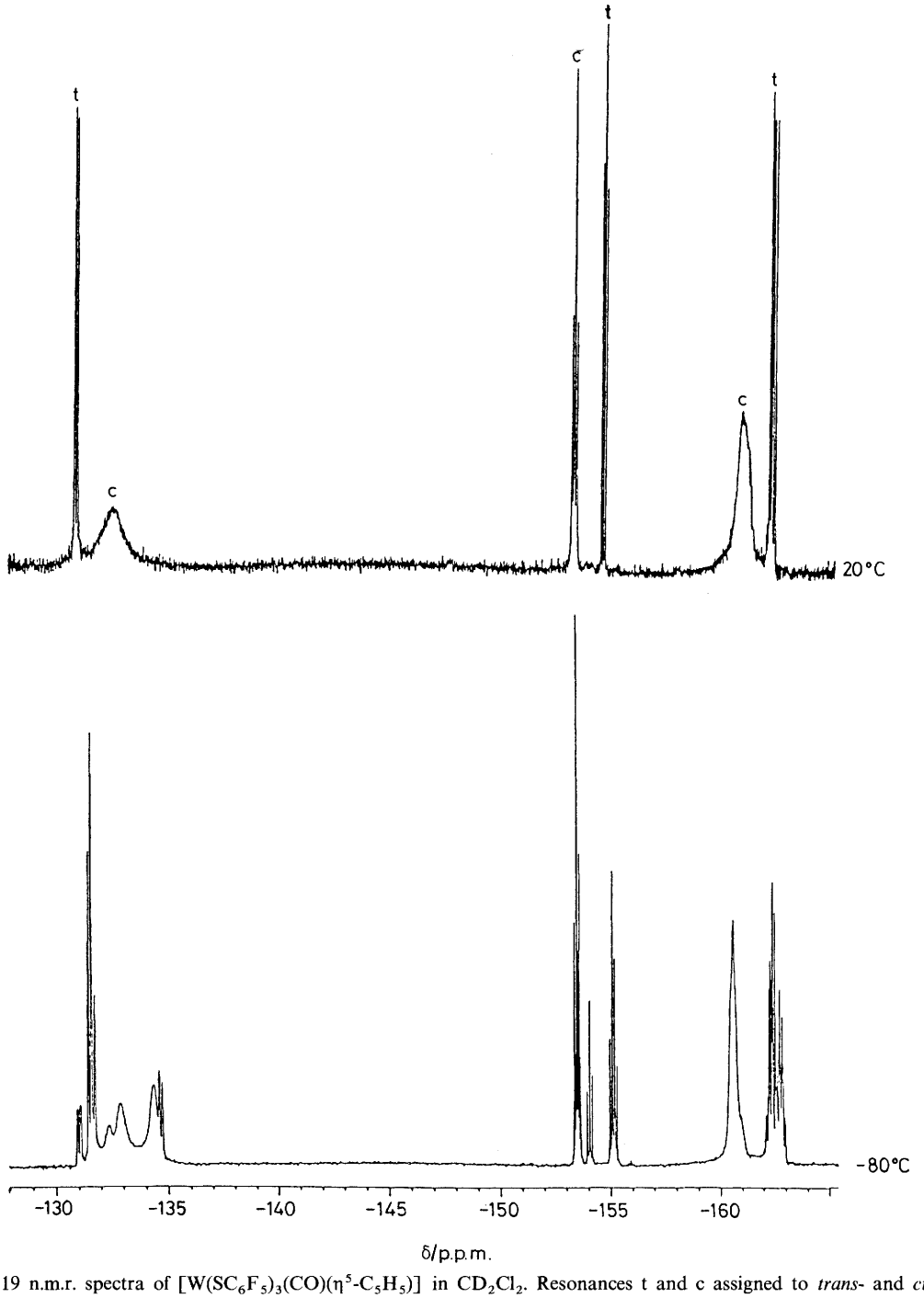

Figure 3. Fluorine-19 n.m.r. spectra of $[W(SC_6F_5)_3(CO)(\eta^5\text{-}C_5H_5)]$ in CD_2Cl_2. Resonances t and c assigned to *trans*- and *cis*-C_6F_5 groups, respectively

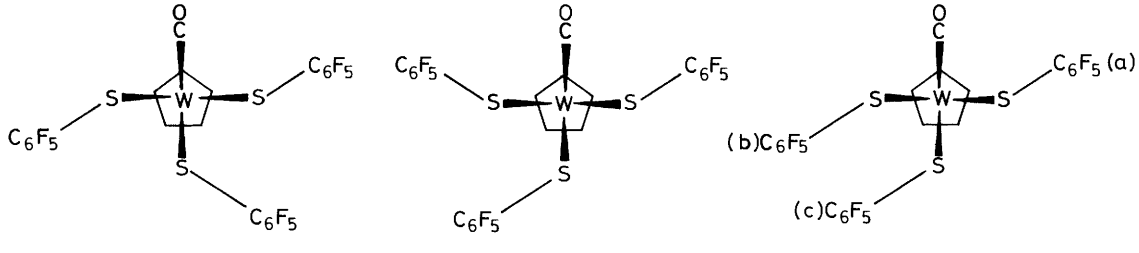

(3i) (3ii) (3iii)

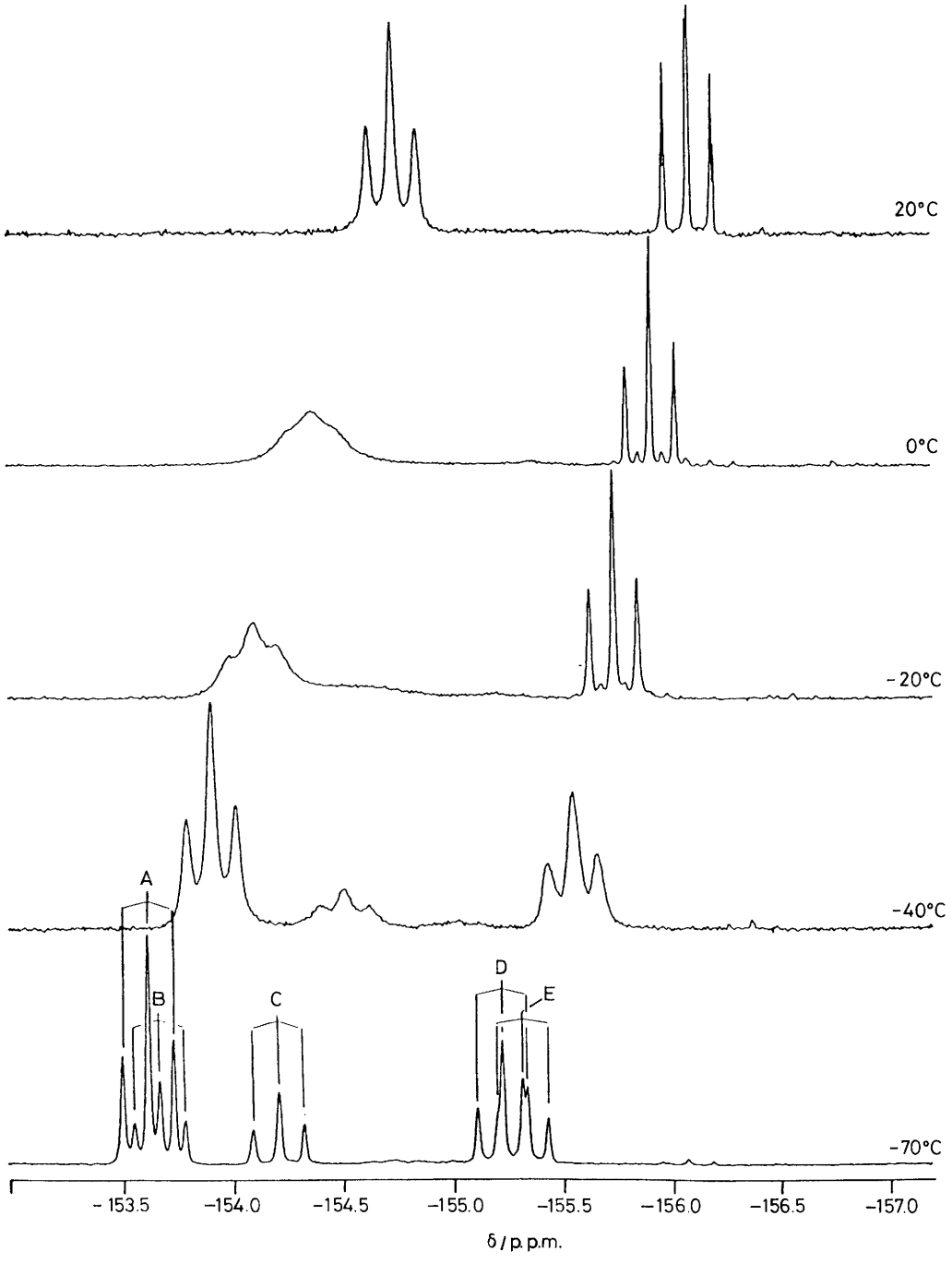

Figure 4. Variable-temperature ^{19}F n.m.r. spectra of $[W(SC_6F_5)_3(CO)(\eta^5\text{-}C_5H_5)]$ (**3**) in CD_2Cl_2 showing the *para*-fluorine resonances

case of the *trans* sulphur. It is therefore to be expected that the barrier to rotation of the *trans*-C_6F_5S ligand about the W–S bond will be lower than that of the *cis* ligands since the electronic origin of the barrier is the directional nature of W–S π bonding.

The major product of the reaction between $[WBr_3(CO)_2(\eta^5\text{-}C_5H_5)]$ and excess of $Tl(SC_6F_5)$ is the tetrathiolate complex $Tl[W(SC_6F_5)_4(\eta^5\text{-}C_5H_5)]$ (**2b**). It seems probable that this is formed *via* the carbonyl derivative (**3**), the final step in the reaction involving nucleophilic substitution of CO by $C_6F_5S^-$. This is supported by the observation that (**3**) is only ever obtained in small quantities and is not produced at all with prolonged reaction times. A logical sequence of reaction is therefore $[WBr_3(CO)_2(\eta^5\text{-}C_5H_5)] \longrightarrow [W(SC_6F_5)_3(CO)(\eta^5\text{-}C_5H_5)] \longrightarrow Tl[W(SC_6F_5)_4(\eta^5\text{-}C_5H_5)]$. The spectroscopic data for (**2b**) are similar to those of the molybdenum analogue (**2a**) reported previously and consequently a similar structure is proposed. This, as with (**3**), is based on a four-legged piano-stool with in this case four SC_6F_5 groups comprising the square base. In the solid state we assume that the Tl^+ ion is co-ordinated by the four sulphurs and lies distal to the $\eta^5\text{-}C_5H_5$ ligand. *X*-Ray diffraction studies of complex (**2a**) also revealed the presence of close contacts between the thallium ion and four of the eight *ortho*-fluorines of the C_6F_5 groups. The latter clearly adopt a preferred orientation in the solid state and contribute to a co-ordination pocket in the $[Mo(SC_6F_5)_4(\eta^5\text{-}C_5H_5)]^-$ anion which partially encapsulates the thallium cation.

Dynamic ^{19}F n.m.r. data for (**2b**) as with (**2a**) indicate that

Table 3. Fractional co-ordinates of atoms with standard deviations for complex (**4b**)

Atom	*x*	*y*	*z*	Atom	*x*	*y*	*z*
Mo	1.190 64(4)	0.416 06(4)	0.210 80(2)	F(22)	1.504 47(19)	0.442 96(18)	0.427 99(10)
S(1)	1.116 70(14)	0.518 69(12)	0.112 19(7)	F(23)	1.380 31(19)	0.334 96(18)	0.379 93(10)
C(1)	0.983 22(17)	0.392 76(14)	0.076 29(9)	C(61)	1.296 2(5)	0.244 7(4)	0.242 31(19)
C(2)	0.880 91(17)	0.379 32(14)	0.056 49(9)	C(62)	1.378 5(5)	0.312 1(4)	0.231 15(19)
C(3)	0.782 20(17)	0.464 76(14)	0.045 39(9)	C(63)	1.391 6(5)	0.354 2(4)	0.164 94(19)
C(4)	0.785 78(17)	0.563 62(14)	0.054 13(9)	C(64)	1.317 5(5)	0.312 9(4)	0.135 18(19)
C(5)	0.888 08(17)	0.577 03(14)	0.073 96(9)	C(65)	1.258 5(5)	0.245 3(4)	0.182 99(19)
C(6)	0.986 81(17)	0.491 61(14)	0.085 03(9)	P(1)	0.769 5(14)	0.014 92(12)	0.239 37(7)
F(1)	1.079 42(17)	0.309 50(14)	0.087 11(9)	N	0.746 7(5)	−0.058 7(4)	0.305 02(23)
F(2)	0.877 43(17)	0.282 99(14)	0.047 97(9)	P(2)	0.678 36(14)	−0.145 97(12)	0.343 03(7)
F(3)	0.682 50(17)	0.451 68(14)	0.026 09(9)	C(25)	0.688 1(4)	0.170 3(3)	0.312 99(16)
F(4)	0.689 57(17)	0.646 88(14)	0.043 34(9)	C(26)	0.653 9(4)	0.274 7(3)	0.324 13(16)
F(5)	0.891 58(17)	0.673 37(14)	0.082 46(9)	C(27)	0.651 3(4)	0.360 0(3)	0.273 13(16)
S(2)	1.256 54(16)	0.574 18(14)	0.212 01(7)	C(28)	0.683 0(4)	0.340 9(3)	0.210 98(16)
C(7)	1.144 72(18)	0.739 76(16)	0.122 81(9)	C(29)	0.717 2(4)	0.236 5(3)	0.199 83(16)
C(8)	1.140 64(18)	0.810 65(16)	0.065 99(9)	C(30)	0.719 8(4)	0.151 2(3)	0.250 84(16)
C(9)	1.244 09(18)	0.808 13(16)	0.022 88(9)	C(31)	0.744 5(3)	−0.081 8(3)	0.143 88(19)
C(10)	1.351 62(18)	0.734 73(16)	0.036 60(9)	C(32)	0.679 1(3)	−0.102 6(3)	0.101 08(19)
C(11)	1.355 70(18)	0.663 85(16)	0.093 42(9)	C(33)	0.560 3(3)	−0.041 8(3)	0.092 92(19)
C(12)	1.252 25(18)	0.666 37(16)	0.136 52(9)	C(34)	0.506 9(3)	0.039 7(3)	0.127 56(19)
F(7)	1.043 91(18)	0.742 20(16)	0.164 81(9)	C(35)	0.572 3(3)	0.060 4(3)	0.170 36(19)
F(8)	1.035 85(18)	0.882 17(16)	0.052 62(9)	C(36)	0.691 1(3)	−0.000 3(3)	0.178 52(19)
F(9)	1.240 11(18)	0.877 21(16)	−0.032 48(9)	C(37)	1.013 0(4)	−0.080 2(3)	0.252 51(17)
F(10)	1.452 43(18)	0.732 29(16)	−0.005 40(9)	C(38)	1.138 6(4)	−0.095 4(3)	0.233 79(17)
F(11)	1.460 50(18)	0.592 33(16)	0.106 79(9)	C(39)	1.181 2(4)	−0.040 1(3)	0.175 63(17)
S(3)	0.993 02(14)	0.374 69(13)	0.227 73(7)	C(40)	1.098 2(4)	0.030 4(3)	0.136 18(17)
C(13)	1.002 09(21)	0.192 21(17)	0.319 60(10)	C(41)	0.972 5(4)	0.045 7(3)	0.154 90(17)
C(14)	0.974 23(21)	0.135 31(17)	0.378 91(10)	C(42)	0.929 9(4)	−0.009 6(3)	0.213 06(17)
C(15)	0.902 64(21)	0.187 37(17)	0.425 59(10)	C(43)	0.851 8(4)	−0.192 0(3)	0.424 46(20)
C(16)	0.858 91(21)	0.296 33(17)	0.412 98(10)	C(44)	0.919 9(4)	−0.254 6(3)	0.473 10(20)
C(17)	0.886 75(21)	0.353 23(17)	0.353 67(10)	C(45)	0.909 0(4)	−0.358 7(3)	0.497 33(20)
C(18)	0.958 35(21)	0.301 16(17)	0.306 99(10)	C(46)	0.830 0(4)	−0.400 2(3)	0.472 94(20)
F(13)	1.071 83(21)	0.141 49(17)	0.274 11(10)	C(47)	0.762 0(4)	−0.337 6(3)	0.424 31(20)
F(14)	1.016 83(21)	0.029 12(17)	0.391 20(10)	C(48)	0.772 8(4)	−0.233 5(3)	0.400 07(20)
F(15)	0.875 49(21)	0.131 90(17)	0.483 40(10)	C(49)	0.469 4(4)	0.014 0(4)	0.363 22(19)
F(16)	0.789 14(21)	0.347 04(17)	0.458 49(10)	C(50)	0.362 6(4)	0.016 0(4)	0.398 53(19)
F(17)	0.844 15(21)	0.459 40(17)	0.341 38(10)	C(51)	0.325 3(4)	0.007 7(4)	0.458 51(19)
S(4)	1.144 39(15)	0.418 37(15)	0.324 48(7)	C(52)	0.395 0(4)	−0.092 7(4)	0.483 18(19)
C(19)	1.179 60(19)	0.598 68(18)	0.357 35(10)	C(53)	0.501 8(4)	−0.139 8(4)	0.447 87(19)
C(20)	1.242 49(19)	0.653 38(18)	0.381 69(10)	C(54)	0.539 0(4)	−0.086 4(4)	0.387 89(19)
C(21)	1.351 70(19)	0.601 04(18)	0.405 43(10)	C(55)	0.743 4(3)	−0.296 5(3)	0.267 02(21)
C(22)	1.398 03(19)	0.493 98(18)	0.404 84(10)	C(56)	0.722 1(3)	−0.357 8(3)	0.227 20(21)
C(23)	1.335 14(19)	0.439 30(18)	0.380 51(10)	C(57)	0.602 9(3)	−0.348 0(3)	0.214 98(21)
C(24)	1.225 94(19)	0.491 63(18)	0.356 76(10)	C(58)	0.505 1(3)	−0.276 8(3)	0.242 56(21)
F(19)	1.073 16(19)	0.649 70(18)	0.334 20(10)	C(59)	0.526 4(3)	−0.215 5(3)	0.282 38(21)
F(20)	1.197 32(19)	0.757 71(18)	0.382 25(10)	C(60)	0.645 6(3)	−0.225 4(3)	0.294 61(21)
F(21)	1.412 97(19)	0.654 34(18)	0.429 15(10)				

this structure is retained in [$^2H_8$]toluene at −80 °C since one *para*-, two *ortho*-, and two *meta*-fluorine resonances are observed. One of the *ortho* resonances exhibits distinct Tl–F spin–spin coupling (J_{TlF} = 3 537 Hz) consistent with the proposed solid-state structure. At higher temperatures the peaks broaden and collapse to give one *meta*- and one *para*-fluorine resonance and a broad unresolved *ortho*-fluorine signal at room temperature. This is interpreted in terms of the onset of free rotation of the C_6F_5 groups about the C–S bond combined with dissociation of the Tl^+ ion from the 1:1 complex. This occurs more readily in [$^2H_6$]acetone since three sharp resonances are obtained at 20 °C suggesting that Tl^+ dissociation is essentially complete and that C_6F_5 rotation is rapid on the n.m.r. timescale at this temperature. These data are comparable to those obtained for complex (**2a**) where similar conclusions were reached. Although we have no means of detecting rotation about the M–S bonds in (**2a**) and (**2b**) it seems likely that as with (**3**) this does occur at higher temperatures. As with (**3**) molecular graphics studies of (**2a**) established that completely free rotation of the C_6F_5 groups about the C–S bond is precluded by steric interactions between the *ortho*-fluorines and the nearest adjacent sulphur atom. Thus, rotation about the C_6F_5–S bonds probably requires at least partial rotation about the M–S bond or deformation (inversion) of the M–S–C bond system. Moreover, for this to occur a concerted motion of all four C_6F_5S groups is probably required in order to prevent C_6F_5–C_6F_5 interactions of the type described for [$W(SC_6F_5)_3(CO)(\eta^5$-$C_5H_5)$], isomer (**3iii**).

In view of the evidence obtained for dissociation of Tl^I in solutions of complexes (**1**), (**2a**), and (**2b**) it was of interest to replace the thallium ion in these derivatives by a non-co-ordinating cation. This was readily achieved by reaction of (**2a**), (**2b**), and (**1**) with $NMe_4^+Cl^-$, $NBu^n{}_4^+Br^-$, or $N(PPh_3)_2^+Cl^-$ at room temperature in dichloromethane solution. In this way [X][$Mo(SC_6F_5)_4(\eta^5$-$C_5H_5)$] [X = $NBu^n{}_4$ (**4a**) or $N(PPh_3)_2$ (**4b**)], [NMe_4][$W(SC_6F_5)_4(\eta^5$-$C_5H_5)$] (**4c**), and [$N(PPh_3)_2$],

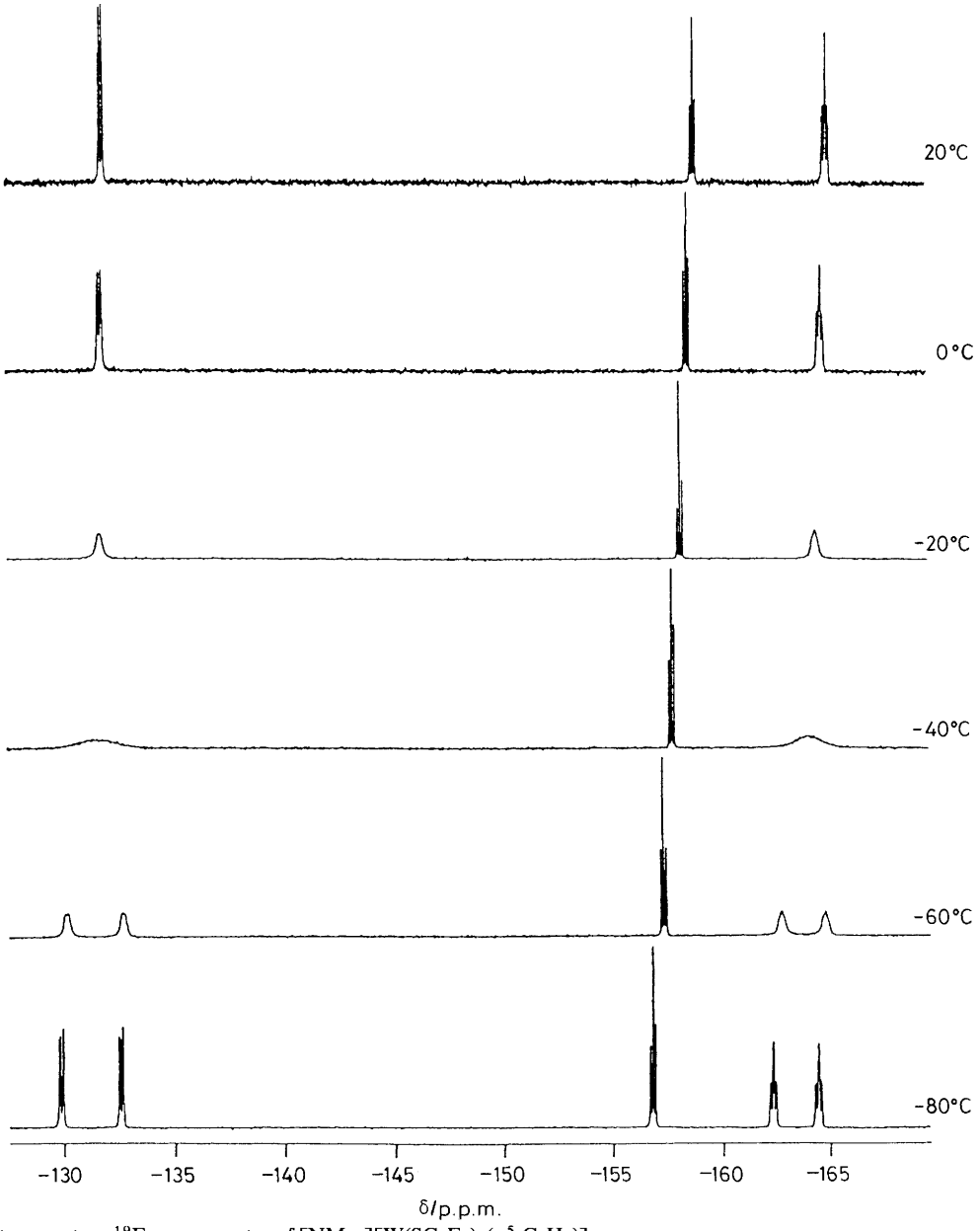

Figure 5. Variable-temperature ^{19}F n.m.r. spectra of $[NMe_4][W(SC_6F_5)_4(\eta^5\text{-}C_5H_5)]$

and $[Mo(SC_6F_5)_2(CO)_2(\eta^5\text{-}C_5H_5)]$ (**5**) were isolated in *ca.* 60—70% yield. The tetrathiolates are orange (**4a**), (**4b**), or yellow (**4c**) crystalline complexes, soluble in polar organic solvents and reasonably air stable in the solid state. The dicarbonyl (**5**) exhibits higher solubility but is also more air sensitive, particularly in solution. The complexes exhibit some spectroscopic similarities to their thallium(I) precursors although differences are also apparent, reflecting the inability of the nitrogen-based cations to co-ordinate to the organometallic anion.

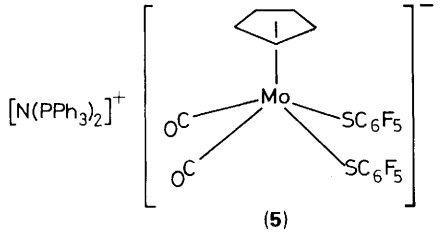

(**5**)

Complex (**5**) shows two ν(CO) modes in the i.r. spectrum at 1 930 and 1 830 cm^{-1} ($CHCl_3$) similar to those of the thallium derivative (**1**) and therefore consistent with the illustrated *cis* structure. However, unlike complex (**1**) the ^{19}F n.m.r. spectrum is temperature invariant showing one set of C_6F_5 resonances down to −80 °C in CD_2Cl_2. Since, under the same conditions, evidence was found for preferred C_6F_5 orientations as well as thallium ion dissociation in complex (**1**) it appears that restricted rotation about the C_6F_5–S bond is a direct consequence of co-ordination of Tl^I with the thiolate sulphurs. It did not prove possible to obtain crystals of (**5**) suitable for *X*-ray diffraction studies but molecular graphics studies of $Tl[Mo(SC_6F_5)_2(CO)_2(\eta^5\text{-}C_5H_5)]$ established that the only steric impediment to C_6F_5 rotation is contact between the *ortho*-fluorines and the thallium. In agreement with the n.m.r. data for (**5**) removal of thallium allows free rotation.

Dynamic ^{19}F n.m.r. studies of the tetrathiolates (**4a**)—(**4c**), in contrast, revealed that free rotation only occurs at 20 °C (see Figure 5) where the sharp fluorine peaks are observed but at lower temperatures both the *ortho* and *meta* signals split into

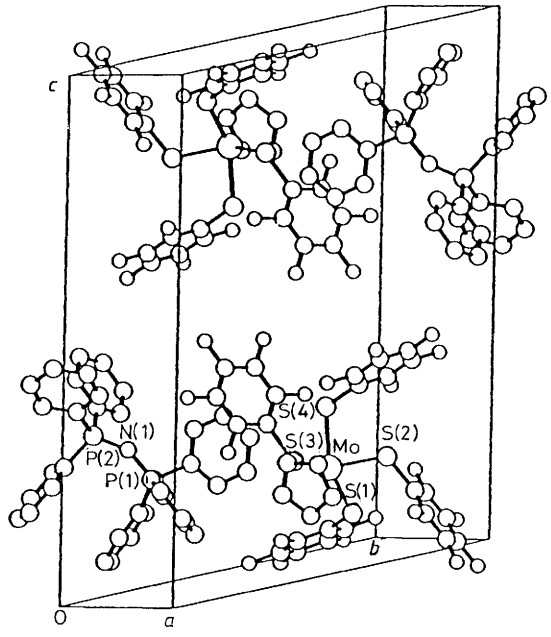

Figure 6. Crystal packing diagram for complex (**4b**) (PLUTO[17])

Table 4. Selected derived geometrical parameters (lengths in Å, angles in °) with standard deviations for complex (**4b**)

Mo–S(1)	2.417 0(16)	S(3)–C(18)	1.818(3)
Mo–S(2)	2.414 4(18)	S(4)–C(24)	1.816(3)
Mo–S(3)	2.412 3(17)	P(1)–N	1.565(5)
Mo–S(4)	2.436 9(18)	P(1)–C(30)	1.799(4)
Mo–C(61)	2.278(5)	P(1)–C(36)	1.785(4)
Mo–C(62)	2.267(5)	P(1)–C(42)	1.786(4)
Mo–C(63)	2.345(5)	N–P(2)	1.574(5)
Mo–C(64)	2.401(5)	P(2)–C(48)	1.783(5)
Mo–C(65)	2.361(5)	P(2)–C(54)	1.799(5)
S(1)–C(6)	1.828(3)	P(2)–C(60)	1.780(5)
S(2)–C(12)	1.814(3)		
S(1)–Mo–S(2)	82.97(6)	S(4)–C(24)–C(19)	120.55(18)
S(1)–Mo–S(3)	82.23(6)	S(4)–C(24)–C(23)	119.46(18)
S(1)–Mo–S(4)	138.64(6)	N–P(1)–C(30)	108.06(24)
S(2)–Mo–S(3)	133.58(6)	N–P(1)–C(36)	113.95(24)
S(2)–Mo–S(4)	81.47(6)	N–P(1)–C(42)	109.85(25)
S(3)–Mo–S(4)	81.35(6)	C(30)–P(1)–C(36)	108.71(19)
Mo–S(1)–C(6)	119.32(10)	C(30)–P(1)–C(42)	107.01(20)
S(1)–C(6)–C(1)	123.91(16)	C(36)–P(1)–C(42)	109.02(20)
S(1)–C(6)–C(5)	116.09(15)	P(1)–N–P(2)	145.6(4)
Mo–S(2)–C(12)	113.55(10)	N–P(2)–C(48)	108.56(25)
S(2)–C(12)–C(7)	119.47(16)	N–P(2)–C(54)	110.9(3)
S(2)–C(12)–C(11)	120.52(17)	N–P(2)–C(60)	114.0(3)
Mo–S(3)–C(18)	113.54(10)	C(48)–P(2)–C(54)	106.03(22)
S(3)–C(18)–C(13)	119.37(18)	C(48)–P(2)–C(60)	107.48(21)
S(3)–C(18)–C(17)	120.60(18)	C(54)–P(2)–C(60)	109.54(22)
Mo–S(4)–C(24)	116.57(11)		

two equal-intensity resonances to give a stereochemically rigid system in each case at −80 °C. Clearly a barrier to rotation is still present despite the removal of thallium from the complexes. Consequently *X*-ray diffraction studies of (**4b**) were carried out with a view to (*a*) establishing the origin of the barrier and (*b*) defining the structural effects of thallium co-ordination on the anion $[Mo(SC_6F_5)_4(\eta^5\text{-}C_5H_5)]^-$ by comparison with (**2a**).

Solid-state Structure of $[N(PPh_3)_2][Mo(SC_6F_5)_4(\eta^5\text{-}C_5H_5)]$.—Orange-red crystals of complex (**4b**), obtained from dichloromethane–hexane at −15 °C, were subjected to structural analysis by *X*-ray diffraction. The lattice contains discrete ions $[(Ph_3P)N(PPh_3)]^+$ and $[Mo(SC_6F_5)_4(\eta^5\text{-}C_5H_5)]^-$ with closest interionic contacts between H and F being >2.5 Å and between C and F being >2.85 Å. A packing diagram, Figure 6, indicates the distribution of ionic species. An ORTEP[11] diagram of the structure of $[Mo(SC_6F_5)_4(\eta^5\text{-}C_5H_5)]^-$ is given in Figure 7 and Tables 3 and 4 list, respectively, the atomic fractional co-ordinates and selected, derived geometrical parameters for this anion.

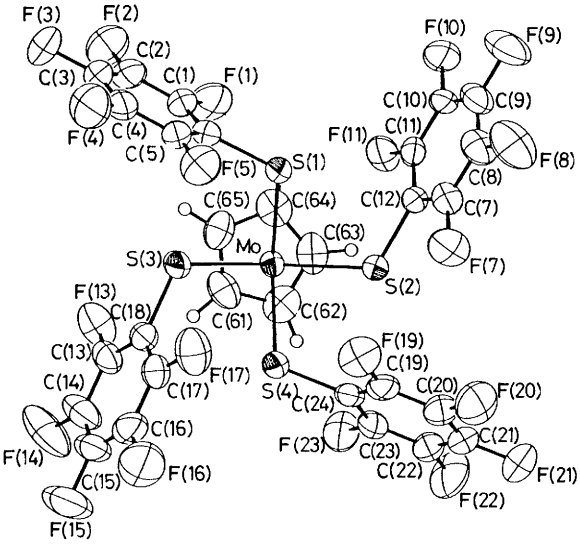

Figure 7. Molecular structure of complex (**4b**) (ORTEP[11])

The 'piano-stool' geometry of $[Mo(SC_6F_5)_4(\eta^5\text{-}C_5H_5)]^-$ is very closely related to that of $Tl[Mo(SC_6F_5)_4(\eta^5\text{-}C_5H_5)]$ (**2a**).[1] The latter contains a Tl^+ ion which occupies a cavity in the anion and interacts with the four S atoms and is closely associated with four *ortho*-F atoms. In complex (**4b**) the anion cavity is vacant. The Mo–S bond lengths in (**4b**) and (**2a**) are essentially the same although there is a small displacement of the S atoms towards the central axis in the latter [mean *trans* angles S–Mo–S: 136.1° in (**4b**), 132.0° in (**2a**)] and this is consistent with co-ordination to Tl^+ in complex (**2a**). The 'swastika-like' arrangement of SC_6F_5 groups around Mo obviates the destabilising interaction between the filled d_{xy} metal orbital and the p_π-donor orbitals on the S atoms and permits a bonding π interaction between the latter orbitals and the unoccupied d_{z^2} orbital, as discussed earlier for complex (**3**).

The fact that the $[Mo(SC_6F_5)_4(\eta^5\text{-}C_5H_5)]^-$ moiety is little altered by deco-ordination of Tl^+ suggests that the variable-temperature n.m.r. data can be explained in terms of the orientation of the SC_6F_5 groups adopted so as to maximise S–M π bonding, and minimise antibonding interactions, Figure 2. As with complexes (**2a**) and (**2b**) at the slow-exchange limit, rotation (or deformation) about the M–S bonds has stopped and consequently the orientation adopted prevents rotation about the C_6F_5–S bonds as a result of steric interaction between the *ortho*-fluorines and an adjacent sulphur atom. At higher temperatures partial concerted rotation (or inversion) about the M–S bonds facilitates C_6F_5 rotation about the C–S bonds. Again we are unable to state unequivocally that complete rotation about the M–S bonds occurs but the fact that this is observed with (**3**) suggests that it is also possible with (**4**). In particular we note that three sulphurs π-donate to one empty metal d_π orbital (d_{z^2}) in complex (**3**) whereas in complexes (**4**), where four sulphurs are involved, M–S π bonding is presumably weaker. On the basis that the electronic barrier to rotation about the M–S bond is thought to result from S→M bonding

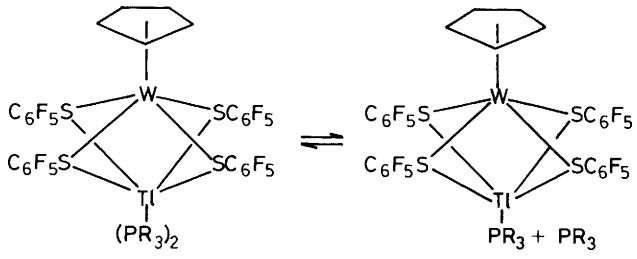

(6i)

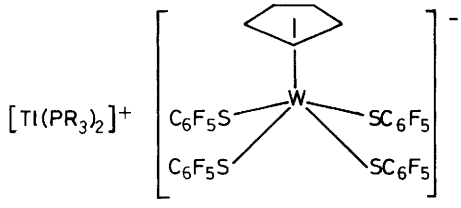

(6ii)

(π) in conjunction with antibonding effects the weaker M–S π bonding should lead to lower barriers to rotation. This is in accord with the reduced coalescence temperatures observed with complexes (**4a**)—(**4c**), *ca.* −40 °C, relative to those of the *cis*-C_6F_5 groups in the ^{19}F n.m.r. spectra of (**3**).

Previously we observed that $Tl[Mo(SC_6F_5)_4(\eta^5\text{-}C_5H_5)]$ forms a 1:2 adduct $Tl[Mo(SC_6F_5)_4(PPh_3)_2(\eta^5\text{-}C_5H_5)]$ (**6a**) on reaction with triphenylphosphine and this exists in two isomeric forms in solution at low temperatures. One form exhibits a ^{19}F n.m.r. spectrum very similar to that of (**2a**), *i.e.* containing distinct thallium–fluorine coupling and hence suggesting structure (**6i**), whereas the other does not show Tl–F coupling and the spectrum is similar to that of complexes (**4**) (see Figure 5). Accordingly structure (**6ii**) was proposed in which phosphine co-ordination to Tl has induced complete dissociation to give a structure containing two ions similar to those of (**4b**). It was therefore of interest to carry out reactions of the tungsten derivative (**2b**) with tertiary phosphines so as to confirm our structural proposals concerning (**6a**).

The reaction of complex (**2b**) with triphenylphosphine in dichloromethane over a period of several days afforded a cloudy yellow solution from which a yellow crystalline solid $Tl[W(SC_6F_5)_4(PPh_3)_2(\eta^5\text{-}C_5H_5)]$ (**6b**) was isolated. Similar reactions with PMe_2Ph and PEt_3 proceeded more rapidly but several recrystallisations of the sticky yellow products were necessary before spectroscopically (n.m.r.) pure samples were obtained in each case. Satisfactory analytical data were obtained only for the PPh_3 derivative (**6b**) although spectroscopic data (^1H and ^{19}F n.m.r.) are fully consistent with the stoicheiometry $[TlW(SC_6F_5)_4L_2(\eta^5\text{-}C_5H_5)]$ in each case [L = PPh_3, PMe_2Ph (**6c**), or PEt_3 (**6d**)]. In particular the ^1H n.m.r. spectrum in each case contains a C_5H_5 singlet and appropriate phosphine resonances, the integrated intensities of which are consistent with the above formula. Moreover the presence of thallium in (**6b**) and (**6c**) was confirmed by *X*-ray fluorescence spectroscopy.

Variable-temperature ^{19}F n.m.r. studies of the triphenylphosphine adduct (**6b**) were carried out over the temperature range +20 to −90 °C in CD_2Cl_2 and [$^2H_6$]acetone. At low temperature in CD_2Cl_2 a 'frozen' spectrum is obtained which is virtually identical to that of the precursor (**2b**) in that one *para*-, two *meta*-, and two *ortho*-fluorine resonances are observed with one of the *ortho* peaks split into a doublet J_{TlF} = 3 479 Hz. As the temperature is raised broadening and collapse of the *ortho* and *meta* resonances occurs to give one sharp *meta* and *para* resonance and a very broad *ortho* signal at 20 °C. Qualitatively the spectra are almost identical to those obtained for (**2b**) but the rate of exchange is greater, *e.g.* the coalescence temperature for the *ortho*-fluorine peaks is *ca.* −35 °C whereas for (**2b**) T_c = −22 °C.

These data are consistent with structure (**6i**) in which the thallium is co-ordinated by the anion $[W(SC_6F_5)_4(\eta^5\text{-}C_5H_5)]^-$ at low temperature and C_6F_5 rotation has been arrested. The $^{31}P\text{-}\{^1H\}$ n.m.r. spectrum shows a singlet resonance at *ca.* 28 p.p.m. which is temperature invariant. This is consistent with co-ordination of one or both phosphines to thallium distal to the tungsten. As suggested previously for (**6a**)[1] the absence of Tl–P coupling suggests an equilibrium involving rapid exchange between free and co-ordinated phosphine.

A comparison of the ^{19}F n.m.r. data for complex (**2b**) and those for (**6b**)—(**6d**) is particularly informative. For example in [$^2H_6$]acetone the spectra of (**2b**) and (**6b**) between +20 and −90 °C are virtually identical indicating that the triphenylphosphines have virtually no kinetic effect whatsoever on thallium dissociation or C_6F_5 rotation. The situation is quite different with the PMe_2Ph and PEt_3 adducts (**6c**) and (**6d**) where the spectra are virtually identical to each other and to that of $[NMe_4][W(SC_6F_5)_4(\eta^5\text{-}C_5H_5)]$ (**4c**) (Figure 5) over the temperature range +20 to −80 °C. Thus, although the C_6F_5 groups adopt a preferred orientation at low temperature, the thallium remains dissociated and no thallium–fluorine coupling is observed. We therefore conclude that the stronger bases PMe_2Ph and PEt_3 bind preferentially with the thallium to the extent that co-ordination by the organometallic anion is not possible. This corresponds to structure (**6ii**). At the other extreme, interaction of the triphenylphosphine ligands in (**6b**) must be very weak and the thallium(I) ion is co-ordinated preferentially by $[W(SC_6F_5)_4(\eta^5\text{-}C_5H_5)]^-$ as in (**6i**). This is essentially the same argument we have employed previously to explain the solvent dependence of the dissociation of Tl^+ from $[Mo(SC_6F_5)_4(\eta^5\text{-}C_5H_5)]^-$, *i.e.* facile dissociation is observed in co-ordinating solvents such as acetone whereas in non-co-ordinating solvents, *e.g.* toluene, dissociation occurs less readily. Moreover, on the basis that $[TlMo(SC_6F_5)_4(PPh_3)_2(\eta^5\text{-}C_5H_5)]$ exists as an equilibrium mixture of the co-ordinated and dissociated forms (**6i**) and (**6ii**) at −90 °C, we conclude that the molybdenum anion $[Mo(SC_6F_5)_4(\eta^5\text{-}C_5H_5)]^-$ forms weaker complexes with $Tl^+/(PPh_3)_2$ than its tungsten analogue.

Experimental

All reactions and manipulations were carried out under an atmosphere of dry oxygen-free nitrogen using standard Schlenk techniques. Solvents were purified as described previously. The starting materials $Tl(SC_6F_5)$,[1] $[WCl(CO)_3(\eta^5\text{-}C_5H_5)]$,[12] $[WBr_3(CO)_2(\eta^5\text{-}C_5H_5)]$,[13] $Tl[Mo(SC_6F_5)_2(CO)_2(\eta^5\text{-}C_5H_5)]$,[1] and $Tl[Mo(SC_6F_5)_4(\eta^5\text{-}C_5H_5)]$[1] were prepared by literature methods. The compounds PPh_3, PMe_2Ph, PEt_3, NMe_4Cl, NBu^n_4Cl, and $N(PPh_3)_2Cl$ were obtained commercially (Strem or Aldrich) and used as supplied.

Proton, ^{19}F, and ^{31}P n.m.r. spectra were recorded on a Bruker WP 200SY at 200.13, 188.31, and 80.32 MHz, respectively, using $SiMe_4$, CCl_3F, and 85% aqueous H_3PO_4 as references (δ = 0.0 p.p.m.). Elemental analyses were carried out at Analytical Laboratories Engelskirchen, West Germany, and at the University of Manchester Institute of Science and Technology.

Reactions.—$[WBr_3(CO)_2(\eta^5\text{-}C_5H_5)]$ *with* $Tl(SC_6F_5)$. The complex (390 mg, 0.72 mmol) and $Tl(SC_6F_5)$ (1 450 mg, 3.60

mmol) were stirred in dichloromethane (40 cm^3) under nitrogen at room temperature for 7 d when the orange solution gradually turned greenish yellow and ultimately yellow-brown. The mixture was filtered, centrifuged, and concentrated *in vacuo*. Hexane (*ca.* 10 cm^3) was added and the solution cooled to −15 °C affording a yellow powder $Tl[W(SC_6F_5)_4(\eta^5\text{-}C_5H_5)]$ (**2b**) and green crystals of $[W(SC_6F_5)_3(CO)(\eta^5\text{-}C_5H_5)]\cdot 0.5\,CH_2Cl_2$ (**3**). These were separated by hand and recrystallised a second time from dichloromethane–hexane to give 300 mg (33%) of (**2b**) and 20 mg (3%) of (**3**) [Found for (**2b**): C, 27.0; H, 0.4; S, 10.6. $C_{29}H_5F_{20}S_4TlW$ requires C, 27.8; H, 0.4; S, 10.3%]. N.m.r.: $^1H(CD_2Cl_2$, 20 °C), δ 5.48 (s, C_5H_5); ^{19}F (CD_2Cl_2, −80 °C), δ −128.20 (dm, J_{TlF} 3 537, 4 *o*-F), −131.46 (t, *J* 31.0, 4 *o*-F), −154.55 (br t, *J* 20.0, 4 *p*-F), −160.82 (t, *J* 23.5, 4 *m*-F), and −162.63 (t, *J* 42.0, 4 *m*-F); [$(CD_3)_2CO$, 20 °C)], −130.76 (br d, *J* 24.0, 8 *o*-F), −160.12 (t, *J* 20.5 Hz, 4 *p*-F), and −165.85 p.p.m. (m, 8*m*-F). Found for (**3**): C, 31.5; H, 0.5; S, 10.4. $C_{24.5}H_6ClF_{15}OS_3W$ requires C, 32.5; H, 0.6; S, 10.7%. I.r. ($CDCl_3$): ν(CO) 2 030s cm^{-1}. N.m.r.: ^1H ($CDCl_3$, 20 °C), δ 5.57 (s, 5 H, C_5H_5) and 5.28 (s, 1 H, CH_2Cl_2); ^{19}F (CD_2Cl_2, 16 °C), δ −128.4 (m), −131.60 (m, 2 *o*-F, *trans*-C_6F_5), −133.54 (br s, 4 *o*-F, *cis*-C_6F_5), −154.51 (br t, *J* 21.0, 2 *p*-F, *cis*-C_6F_5), −156.03 (t, *J* 21.0 Hz, 1 *p*-F, *trans* C_6F_5), −161.88 (br s, 4 *m*-F, *cis*-C_6F_5), −163.35 (m), and −163.95 p.p.m. (m, 2 *m*-F, *trans*-C_6F_5).

$Tl[Mo(SC_6F_5)_4(\eta^5\text{-}C_5H_5)]$ (**2a**) *with* NBu^n_4Br. Complex (**2a**) (160 mg, 0.14 mmol) and NBu^n_4Br (60 mg 0.19 mmol) in dichloromethane (40 cm^3) were stirred under nitrogen for 5 min when the solution turned cloudy. The mixture was filtered, hexane (10 cm^3) added, and concentrated *in vacuo* to give orange crystals. These were recrystallised from dichloromethane–hexane to give $[NBu^n_4][Mo(SC_6F_5)_4(\eta^5\text{-}C_5H_5)]$ (**4a**) (120 mg, 73%) (Found: C, 44.3; H, 3.6; N, 1.5. $C_{45}H_{41}F_{20}MoNS$ requires C, 45.0; H, 3.4; N, 1.2%). N.m.r.: $^1H(CDCl_3)$, δ 5.27 (s, 5 H, C_5H_5), 3.11 (m, 8 H, CH_2), 1.60 (m, 8 H, CH_2), 1.39 (m, 8 H, CH_2), and 0.96 (t, *J* 1.2 Hz, 12 H, Me); ^{19}F (CD_2Cl_2, 20 °C), δ −131.37 (m, 8 *o*-F), −160.10 (t, *J* 21.5, 4 *p*-F), and −166.0 (m, 8 *m*-F); (CD_2Cl_2, 80 °C), −129.45 (m, 4 *o*-F), −132.87 (m, 4 *o*-F), −157.10 (t, *J* 22.0, 4 *p*-F), −162.89 (br t, 23.0, 4 *m*-F), and −164.54 p.p.m. (br t, *J* 23.0 Hz, 4 *m*-F).

$Tl[Mo(SC_6F_5)_4(\eta^5\text{-}C_5H_5)]$ (**2a**) *with* $N(PPh_3)_2Cl$. Complex (**2a**) (80 mg, 0.07 mmol) and $N(PPh_3)_2Cl$ (50 mg, 0.09 mmol) in dichloromethane (40 cm^3) were stirred under nitrogen for 15 min. Work up as for (**4a**) gave orange crystals of $[N(PPh_3)_2][Mo(SC_6F_5)_4(\eta^5\text{-}C_5H_5)]$ (**4b**) (72 mg, 70%) (Found: C, 51.1; H, 2.2; N, 0.8. $C_{65}H_{35}F_{20}MoNP_2S_4$ requires C, 52.2; H, 2.3; N, 0.8%). N.m.r.: ^1H, (CD_2Cl_2, 20 °C); δ 7.4—7.65 (m, 30 H, C_6H_5), and 5.24 (s, 5 H, C_5H_5); ^{19}F (CD_2Cl_2, 20 °C), δ 131.28 (m, 8 *o*-F), −160.07 (t, *J* 21.0, 4 *p*-F), and −166.03 (m, 8, *m*-F); (CD_2Cl_2, −80 °C), −129.24 (m, 4 *o*-F), −133.07 (m, 4 *o*-F), −157.53 (t, *J* 22.0 Hz, 4 *p*-F), −163.32 (m, 4 *m*-F), and −164.68 p.p.m. (m, 4 *m*-F).

$Tl[W(SC_6F_5)_4(\eta^5\text{-}C_5H_5)]$ (**2b**) *with* NMe_4Cl. Complex (**2b**) (90 mg, 0.07 mmol) and NMe_4Cl (20 mg, 0.18 mmol) in dichloromethane (40 cm^3) were stirred under nitrogen for 1.5 h. Work up as for (**4a**) gave a yellow microcrystalline solid $[NMe_4][W(SC_6F_5)_4(\eta^5\text{-}C_5H_5)]$ (**4c**) (60 mg, 74%) (Found: C, 34.4; H, 1.5; N, 1.2. $C_{33}H_{17}F_{20}NS_4W$ requires C, 35.4; H, 1.5; N, 1.3%). N.m.r. (CD_2Cl_2): ^1H (20 °C), δ 5.05 (s, 5 H, C_5H_5) and 3.24 (s, 12 H, Me); ^{19}F (CD_2Cl_2, 20 °C), −131.85 (m, 8 *o*-F), −158.91 (t, *J* 21.0, 4 *p*-F), −164.89 (m, 8 *m*-F); (−80 °C), −129.94 (m, 4 *o*-F), −132.56 (m, 4 *o*-F), −156.84 (t, *J* 22.0, 4 *p*-F), −162.37 (t, *J* 23.0, 4 *m*-F), and −164.46 p.p.m. (t, *J* 23.0 Hz, 4 *m*-F).

$Tl[Mo(SC_6F_5)_2(\eta^5\text{-}C_5H_5)]$ (**1**) *with* $N(PPh_3)_2Cl$. Complex (**1**) (80 mg, 0.1 mmol) and $N(PPh_3)_2Cl$ (65 mg, 0.11 mmol) in dichloromethane (15 cm^3) were stirred under nitrogen for 5 min. Work up as for (**4a**) gave olive crystals of $[N(PPh_3)_2][Mo(SC_6F_5)_2(CO)_2(\eta^5\text{-}C_5H_5)]$ (**5**) (65 mg, 58%) (Found: C, 56.7; H, 3.0; N, 1.4. $C_{55}H_{35}F_{10}MoNO_2P_2S_2$ requires C, 57.2; H, 3.0; N, 1.2%). I.r. ($CHCl_3$): ν(CO) 1 930s and 1 830 ms cm^{-1}. N.m.r. (CD_2Cl_2, 20 °C): ^1H, δ 7.4—7.8 (m, 30 H, Ph) and 5.40 (s, 5 H, C_5H_5); ^{19}F. δ −132.37 (d, *J* 20.0, 4 *o*-F), −164.05 (t, *J* 21.0 Hz, 2 *p*-F), and −166.76 p.p.m. (m, 4 *m*-F).

$Tl[W(SC_6F_5)_4(\eta^5\text{-}C_5H_5)]$ (**2b**) *with Triphenylphosphine*. Complex (**2b**) (30 mg, 0.02 mmol) and triphenylphosphine (0.02 mmol) was stirred in dichloromethane (40 cm^3) under nitrogen at room temperature for 7 d giving a cloudy yellow solution. The mixture was filtered and reduced in volume (*in vacuo*), hexane (*ca.* 10 cm^3) added, and the solution cooled to −15 °C affording yellow crystals of $Tl[W(SC_6F_5)_4(PPh_3)_2(\eta^5\text{-}C_5H_5)]$ (**6b**). A second recrystallisation from dichloromethane–hexane gave 9.30 mg, 22% (Found: C, 43.8; H 2.0. $C_{65}H_{35}F_{20}P_2S_4TlW$ requires C, 44.0; H, 2.0%). N.m.r.: ^1H (CD_2Cl_2, 20 °C), δ 7.40—7.70 (m, 30 H, C_6H_5) and 5.45 (s, 5 H, C_5H_5); ^{19}F [$(CD_3)_2CO$, 20 °C], δ −130.74 (br d, *J* 23.0, 8 *o*-F), −160.30 (t, *J* 20.5, 4 *p*-F), and −165.97 (m, 8 *m*-F); (CD_2Cl_2, −80 °C), δ −127.80 (d, J_{TlF} 3 479 Hz, 4 *o*-F), −131.61 (br s, 4 *o*-F), −154.85 (br s, 4 *p*-F), −161.04 (br s, 4 *m*-F) and −162.79 p.p.m. (br s, 4 *m*-F).

$Tl[W(SC_6F_5)_4(\eta^5\text{-}C_5H_5)]$ (**2b**) *with Dimethylphenylphosphine*. Complex (**2b**) 30 mg, 0.02 mmol) was dissolved in dichloromethane (40 cm^3) and nitrogen was bubbled through for 5 min. Dimethylphenylphosphine (3.3 mg, 0.02 mmol) in dichloromethane (2 cm^3) was added dropwise to the solution and stirred under nitrogen at room temperature for 3 h giving a cloudy yellow solution. The mixture was filtered and reduced in volume (*in vacuo*), hexane (*ca.* 10 cm^3) added, and the solution cooled to −15 °C affording greenish yellow crystals (10 mg, 27%) of crude $Tl[W(SC_6F_5)_4(PMe_2Ph)_2(\eta^5\text{-}C_5H_5)]$ (**6c**). Three further recrystallisations from dichloromethane–hexane gave a spectroscopically pure sample. N.m.r.: ^1H ($CDCl_3$, 20 °C), δ 7.4—7.8 (m, 10 H, C_6H_5), 5.23 (s, 5 H, C_5H_5), and 2.0 (d, J_{HP} 12.5, 12 H, Me); ^{19}F (CD_2Cl_2, −90 °C), δ −129.52 (m, 4 *o*-F), −132.67 (m, 4 *o*-F), −156.76 (t, *J* 22.0, 4 *p*-F), −162.21 (m, 4 *m*-F), and −164.32 (m, 4 *m*-F); (CD_2Cl_2, 20 °C), δ −131.63 (br d, *J* 23.0, 8 *o*-F), −158.70 (t, *J* 21.0 Hz, 4 *p*-F), and −164.81 (m, 8 *m*-F).

$Tl[W(SC_6F_5)_4(\eta^5\text{-}C_5H_5)]$ (**2b**) *with Triethylphosphine*. Complex (**2b**) (30 mg, 0.02 mmol) was dissolved in dichloromethane (40 cm^3) and nitrogen was bubbled through for 5 min. Triethylphosphine (2.83 mg, 0.02 mmol) in dichloromethane (2 cm^3) was added dropwise to solution and stirred under nitrogen at room temperature for 3 h giving a cloudy yellow solution. The mixture was filtered and reduced in volume (*in vacuo*), hexane (*ca.* 10 cm^3) added, and the solution cooled to −15 °C affording greenish yellow crystals (13 mg, 38%) of crude $Tl[W(SC_6F_5)_4(PEt_3)_2(\eta^5\text{-}C_5H_5)]$ (**6d**). Three further recrystallisations from dichloromethane–hexane gave a spectroscopically pure sample. N.m.r.: ^1H (CD_2Cl_2, 18 °C), δ 5.20 (s, 5 H, C_5H_5) and 1.2—3.0 (overlapping m, 30 H, C_2H_5); ^{19}F (CD_2Cl_2, 18 °C), δ −131.93 (m, 8 *o*-F), −159.36 (t, *J* 21.0, 4 *p*-F), and −165.46 (m, 8 *m*-F); (CD_2Cl_2, −90 °C) δ −129.86 (m, 4 *o*-F), −133.17 (m, 4 *o*-F), −157.14 (t, *J* 22.0 Hz, 4 *p*-F), −162.72 (m, 4 *m*-F), and −164.67 p.p.m. (m, 4 *m*-F).

X-Ray Crystal Structure Determination of the Solvated Tungsten Complex (**3**).—*Crystal data*. $C_{24}H_5F_{15}OS_3W\cdot 0.5CH_2Cl_2$, *M* = 916.6, triclinic, space group $P\bar{1}$ (no. 2), *a* = 9.555 8(10), *b* = 10.560 7(9), *c* = 14.183 1(14) Å, α = 100.690(8), β = 94.846(8), γ = 92.731(8)°, *U* = 1 398.5 $Å^3$, *Z* = 2, D_c = 2.176 g cm^{-3}, D_m = 2.10(5) g cm^{-3} (flotation in methyl iodide–hexane), *F*(000) = 435, μ(Mo-K_α) = 45.51 cm^{-1}, crystal dimensions = 0.35 × 0.25 × 0.5 mm.

Data collection. The intensity data were collected on an Enraf Nonius CAD-4 diffractometer over the hemisphere (*h*: −11 to +11, *k*: 0 to +12, *l*: −16 to +16) in the range 1.0 < θ < 25.0° using ω—2θ scans and Mo-K_α *X*-radiation (λ = 0.710 693 Å).

Of 4 917 unique data, 4 370 were found to have $I > 3\sigma(I)$ and were used in subsequent structure solution and refinement. The data were corrected for Lorentz and polarisation effects and absorption (DIFABS[14]).

Structure solution and refinement. The position of the W atom was readily located on a Patterson map (SHELXS 86[15]) and those of the remaining non-hydrogen atoms of the complex from successive difference Fourier maps. The pentafluorophenyl groups and the cyclopentadienyl group were treated as idealised hexagons (C–C 1.375 and C–F 1.34 Å) and an idealised pentagon (C–C 1.42 and C–H 0.95 Å), respectively. The structure was refined (SHELX 76[16]) using full-matrix least-squares methods with anisotropic thermal parameters for the non-hydrogen atoms. Inspection of the difference Fourier map indicated the presence of a cluster of peaks around the inversion centre at [0.0, 0.5, 0.0] which corresponded to a highly disordered, half molecule of methylene chloride as solvent of crystallisation. The disorder was most successfully modelled using a C–Cl fragment with a highly constrained C–Cl distance (1.74 ± 0.1 Å) and variable occupancy over three sites around the inversion centre. The refined relative occupancies were 0.29:0.10:0.07 (total occupancy 0.46) which is in reasonable agreement with microanalytical data for this complex (see above). At convergence, the discrepancy factors R and R' were 0.031 and 0.040 respectively, where the weighting scheme $w^{-1} = [\sigma^2(F) + 0.000\,243\,F^2]$ gave satisfactory analyses of variance. The final difference Fourier map was essentially featureless apart from a peak *ca.* 1.3 e Å^{-3} near the disordered methylene chloride molecule and three peaks in the range 0.8—1.0 e Å^{-3} in the vicinity of the tungsten atom.

X-*Ray Crystal Structure Determination of the Molybdenum Salt* (**4b**).—*Crystal data.* $[C_{29}H_5F_{20}MoS_4]^-$ $[C_{36}H_{30}NP_2]^+$, M = 1 495.89, orange-red prisms, triclinic, space group $P\bar{1}$ (no. 2), a = 11.407 6(15), b = 13.241 8(14), c = 21.670 8(22) Å, α = 77.400(9), β = 80.387(9), γ = 74.356(10)°, U = 3055.9 Å^3, Z = 2, D_c = 1.625 g cm^{-3}, D_m = 1.69(5) g cm^3 (flotation in bromoform–hexane), $F(000)$ = 1 496, μ(Mo-K_α) = 4.93 cm^{-1}, crystal size *ca.* 0.35 × 0.20 × 0.40 mm.

Data collection. The intensity data were collected over the hemisphere (h: −13 to +13, k: −15 to +15, 1: 0 to +24: $1.0 < \theta < 24.0°$) using ω–2θ scanning and graphite-monochromated Mo-K_α X-radiation (λ = 0.710 693 Å). Of 9 555 unique data measured, 6 422 had $I > 3\sigma(I)$ and were subsequently used in structure solution and refinement. The data were corrected for Lorentz and polarisation effects, and for absorption (DIFABS[14]).

Structure solution and refinement. The positions of the heavy atoms, Mo, P, and S, were found from a Patterson map (SHELXS 86[15]) and the remainder of the complex from successive difference Fourier maps. The pentafluorophenyl (C–C 1.375 and C–F 1.34 Å), phenyl (C–C 1.395 and C–H 0.95 Å), and cyclopentadienyl (C–C 1.42 and C–H 0.95 Å) groups were treated as idealised rigid groups with the parameters indicated in parentheses. Blocked-matrix least-squares refinement (SHELX 76[16]) using anisotropic thermal parameters for the non-hydrogen atoms reduced the discrepancy factors R and R' to 0.054 and 0.067 respectively. The weighting scheme $w^{-1} = [\sigma^2(F) + 0.000\,705\,(F^2)]$ gave satisfactory analyses of variance. The final difference Fourier map was essentially featureless with a general noise level *ca.* ±0.25 e Å^{-3} apart from two residual peaks *ca.* 0.9 e Å^{-3} near to the Mo atom.

The computer programs used in this study include DIFABS[14] for empirical absorption correction, SHELXS 86[15] for structure solution, SHELX 76[16] for structure refinement, ORTEP II[11] and PLUTO[17] for plotting, and CALC[18] for incidental crystallographic calculations.

Additional material available from the Cambridge Crystallographic Data Centre comprises the atom co-ordinates, thermal parameters, and remaining bond lengths and angles.

Acknowledgements

We thank Professor M. B. Hursthouse, QMC, University of London for access to X-ray data collection facilities through the S.E.R.C./QMC X-ray service. We also thank Dr. R. S. Dhariwal for X-ray fluorescence studies.

References

1 W. A. W. A. Bakar, J. L. Davidson, W. E. Lindsell, K. J. McCullough, and K. W. Muir, *J. Chem. Soc., Dalton Trans.*, 1989, 991; *J. Organomet. Chem.*, 1987, **322**, C1.
2 J. L. Davidson, *J. Chem. Soc., Dalton Trans.*, 1986, 2423 and refs. therein.
3 K. W. Barnett and D. W. Slocum, *J. Organomet. Chem.*, 1972, **44**, 1.
4 P. Kubacek, R. Hoffmann, and Z. Havlas, *Organometallics*, 1982, **1**, 180.
5 C. Bueno and M. R. Churchill, *Inorg. Chem.*, 1981, **20**, 2197.
6 B. S. Erler, J. C. Dewan, S. J. Lippard, and D. R. Tyler, *Inorg. Chem.*, 1981, **20**, 2719.
7 M. L. Listemann, J. C. Dewan, and R. R. Schrock, *J. Am. Chem. Soc.*, 1985, **107**, 207.
8 J. L. Davidson, W. F. Wilson, and K. W. Muir, *J. Chem. Soc., Chem. Commun.*, 1985, 460; T. Debaerdemaeker and A. Kotoglu, *Acta Crystallogr., Sect. B*, 1973, **29**, 2664; O. A. Rajan, M. McKenna, J. Noordik, R. C. Haltiwanger, and M. Rakowski-Dubois, *Organometallics*, 1984, **3**, 831; N. M. Agh-Atabay, J. L. Davidson, G. Douglas, and K. W. Muir, *J. Chem. Soc., Chem. Commun.*, 1989, 549.
9 J. L. Davidson, *J. Chem. Soc., Dalton Trans.*, 1986, 2423.
10 Chem-X, Chemical Design Ltd., Oxford 1987.
11 C. K. Johnson, Report ORNL-5183, Oak Ridge National Laboratory, Tennessee, 1976.
12 T. S. Piper and G. Wilkinson, *J. Inorg. Nucl. Chem.*, 1956, **3**, 104.
13 J. L. Davidson and G. Vasapollo, *J. Organomet. Chem.*, 1985, **291**, 43.
14 N. G. Walker and D. Stuart, *Acta Crystallogr., Sect. A*, 1983, **39**, 158.
15 G. M. Sheldrick, University of Göttingen, 1986.
16 G. M. Sheldrick, University Chemical Laboratory, Cambridge, 1976.
17 S. Motherwell, University Chemical Laboratory, Cambridge, 1976.
18 R. O. Gould and P. Taylor, University of Edinburgh, 1973.

Received 20*th December* 1988; *Paper* 8/04979C